

Antiferromagnetic complexes with metal–metal bonds.  
Part XXX. Synthesis and molecular structures of the  
antiferromagnetic adducts  $[\text{Cp}'\text{Cr}(\mu\text{-SPh})]_2(\mu_3\text{-Se})\cdot\text{ML}$  ( $\text{Cp}' = \eta^5\text{-CH}_3\text{C}_5\text{H}_4$ ,  $\text{ML} = \text{Fe}_3(\mu_3\text{-S})_2(\text{CO})_8$ ,  $\text{Mn}_2(\text{CO})_9$ ,  $\text{Mn}_2(\text{CO})_8$ ),  
paramagnetic complexes  $\text{Cp}'\text{Cr}(\mu\text{-SPh})_3\text{Mn}(\text{CO})_3$  and  $[\text{Cp}'\text{Cr}(\mu\text{-SPh})]_2\text{Te}$ , diamagnetic cluster  $\text{Cp}'_2\text{Cr}_2(\mu\text{-SPh})(\mu_3\text{-S})(\mu_3\text{-Te})\text{Co}(\text{CO})_2$ <sup>☆</sup>

A.A. Pasynskii<sup>a,\*</sup>, I.V. Skabitski<sup>a</sup>, Yu.V. Torubaev<sup>a</sup>, N.I. Semenova<sup>a</sup>,  
V.M. Novotortsev<sup>a</sup>, O.G. Ellert<sup>a</sup>, K.A. Lyssenko<sup>b</sup>

<sup>a</sup> N.S. Kurnakov Institute of General and Inorganic Chemistry RAS, 31 Leninsky Prosp. Moscow GSP-1, 119991, Russia

<sup>b</sup> A.N. Nesmeyanov Institute of Organoelement Compounds RAS, 28 Vavilova str., Moscow V-334, 117813, Russia

Received 31 October 2002; received in revised form 9 January 2003; accepted 9 January 2003

## Abstract

The photochemical reactions of antiferromagnetic heterochalcogenic complex  $[\text{Cp}'\text{Cr}(\mu\text{-SPh})]_2(\mu\text{-Se})$  (**1**) ( $\text{Cp}' = \eta^5\text{-CH}_3\text{C}_5\text{H}_4$ ) with  $\text{Fe}_3(\mu_3\text{-Se})_2(\text{CO})_9$  or  $\text{Mn}_2(\text{CO})_{10}$  at room temperature gives new mixed-metal heterochalcogenic clusters  $[\text{Cp}'\text{Cr}(\mu\text{-SPh})]_2(\mu_3\text{-Se})\text{Fe}_3(\mu_3\text{-Se})_2(\text{CO})_8$  (**2**),  $[\text{Cp}'\text{Cr}(\mu\text{-SPh})]_2(\mu_3\text{-Se})\text{Mn}_2(\text{CO})_9$  (**3**) and  $[\text{Cp}'\text{Cr}(\mu\text{-SPh})]_2(\mu_4\text{-Se})\text{Mn}_2(\text{CO})_8$  (**4**) which are antiferromagnetic ( $-2J = 256, 230$  and  $324 \text{ cm}^{-1}$ , respectively) and characterized by X-ray diffraction analysis (**2**: Cr–Cr 2.763(1) Å; Fe–Fe 2.6184(9) and 2.706(1) Å; Cr–Se 2.447, 2.460 Å; **3**: Cr–Cr 2.762 Å; Mn–Mn 2.920 Å; Cr–Se 2.447, 2.460 Å; **4**: Cr–Cr 2.816 Å, Mn–Mn 2.835 Å, Cr–Se 2.464 Å). The photochemical reaction of **1** and  $\text{Mn}_2(\text{CO})_{10}$  at higher temperature gives the paramagnetic complex  $\text{Cp}'\text{Cr}(\mu\text{-SPh})_3\text{Mn}(\text{CO})_3$  (**5**) with a weak Cr–Mn bond (3.0239 Å). The new heterochalcogenic complex  $[\text{Cp}'\text{Cr}(\mu\text{-SPh})]_2(\mu\text{-Te})$  (**6**) which obtained at the interaction of  $[\text{Cp}'\text{Cr}(\text{CO})(\mu\text{-SPh})]_2$  with Te and was studied by X-ray method (Cr–Cr 2.772 Å, Cr–S 2.359 Å, Cr–Te 2.601–2.607 Å, Cr–Te–Cr 64.3°), reacted with  $\text{Co}_2(\text{CO})_8$  with formation of the diamagnetic mixed-metal heterochalcogenic cluster  $[\text{Cp}'_2\text{Cr}_2(\text{SPh})(\mu_3\text{-S})(\mu_3\text{-Te})\text{Co}(\text{CO})_2]$  (**7**) (Cr–Cr 2.646 Å, Cr–Co 2.627 Å–2.623 Å, Cr– $\mu_3\text{-S}$  2.282–2.299 Å, Co– $\mu_3\text{-S}$  2.199 Å, Cr– $\mu_3\text{-Te}$  2.630–2.618 Å, Co– $\mu_3\text{-Te}$  2.466 Å, Cr– $\mu\text{-SPh}$  2.335 Å). The role of super-exchange spin–spin interaction through the chalcogen bridge atom is discussed.

© 2003 Elsevier Science B.V. All rights reserved.

**Keywords:** Chromium; Manganese; Cobalt; Iron; Chalcogenide; Cyclopentadienyl complexes; Metal carbonyls; Mixed-metal clusters; Magnetic properties; X-ray analyses

## 1. Introduction

In our preceding researches of antiferromagnetic homo- and heterochalcogenic complexes  $[\eta^5\text{-}(\text{RC}_5\text{H}_4)_2\text{Cr}_2(\mu\text{-SR}')_2](\mu\text{-X})$  where  $\text{R} = \text{CH}_3$ ,  $\text{R}' = \text{Ph}$ ,  $\text{X} = \text{Se}$  [**1**] or  $\text{R} = \text{H}$ ,  $\text{R}' = \text{CMe}_3$ ,  $\text{X} = \text{S}$  [**2**] and their mixed-metal derivatives [**1,3,4**] we observed the significant effect of the chalcogen bridge atom nature on the

<sup>☆</sup> For Part XXIX see Ref. [1].

\* Corresponding author. Tel.: +7-095-954-3841; fax: +7-095-954-1279.

E-mail address: [aapas@rambler.ru](mailto:aapas@rambler.ru) (A.A. Pasynskii).

magnetic properties of clusters. In the investigated clusters the contribution of super-exchange interactions via chalcogenide bridge is comparable to the contributions of direct interactions through Cr–Cr bond [5]. Moreover the substitution of sulphur atom by a bigger selenium atom results in the significant increasing of exchange parameter  $-2J$  from  $430\text{ cm}^{-1}$  for  $[\text{CpCr}(\mu\text{-SCMe}_3)_2(\mu\text{-S})]$  [2] to  $578\text{ cm}^{-1}$  for  $[\text{Cp}^*\text{Cr}(\mu\text{-SPh})_2(\mu\text{-Se})]$  (1) notwithstanding with the elongation of Cr–Cr bond from  $2.689$  to  $2.730\text{ \AA}$  [1]. It was known too that the biggest elongation of the Cr–Cr bond took place at the substitution of sulphur by tellurium atoms: from  $2.676\text{ \AA}$  in  $[\text{CpCr}(\mu\text{-SPh})_2(\mu\text{-S})]$  [6] up to  $2.935\text{ \AA}$  in  $[\text{CpCr}(\mu\text{-TePh})_2(\mu\text{-Te})]$  [7] (the magnetic properties of the last complex were not learned—only a suggestion was done about its paramagnetic activity because of the signal broadening in  $^1\text{H}$ - and  $^{13}\text{C}$ -NMR spectra [7]).

In the case of  $\text{Cp}_2\text{Cr}_2(\mu\text{-SCMe}_3)_2(\mu\text{-S})\text{ML}$  the super-exchange interactions depend strongly upon the type of ML coordination [4,8–11] (see Table 1)

The greatest exchange parameter values were observed in the triangular metal clusters  $\text{Cp}_2\text{Cr}_2(\text{SR})(\mu_3\text{-S})(\mu_3\text{-X})\text{Co}(\text{CO})_2$  ( $\text{X} = \text{S}$ ,  $\text{R} = \text{CMe}_3$ ,  $-2J = 578\text{ cm}^{-1}$  [12];  $\text{X} = \text{Se}$ ,  $\text{R} = \text{Ph}$ ,  $-2J = 692\text{ cm}^{-1}$  [1]).

So we prepared some ML-containing derivatives of 1 on one hand and tellurium-containing complexes  $[\text{Cp}^*\text{Cr}(\mu\text{-SPh})_2(\mu\text{-Te})]$  and  $\text{Cp}_2\text{Cr}_2(\text{SPh})(\mu_3\text{-S})(\mu_3\text{-Te})\text{Co}(\text{CO})_2$  on the other hand to study the influence of ML and chalcogen atom nature on the structures and magnetic properties of clusters.

## 2. Results and discussion

The photochemical interaction between  $[\text{Cp}_2\text{Cr}_2(\mu\text{-SPh})_2(\mu\text{-Se})]$  (1) and  $\text{Fe}_3(\mu_3\text{-Se})_2(\text{CO})_9$  at the room

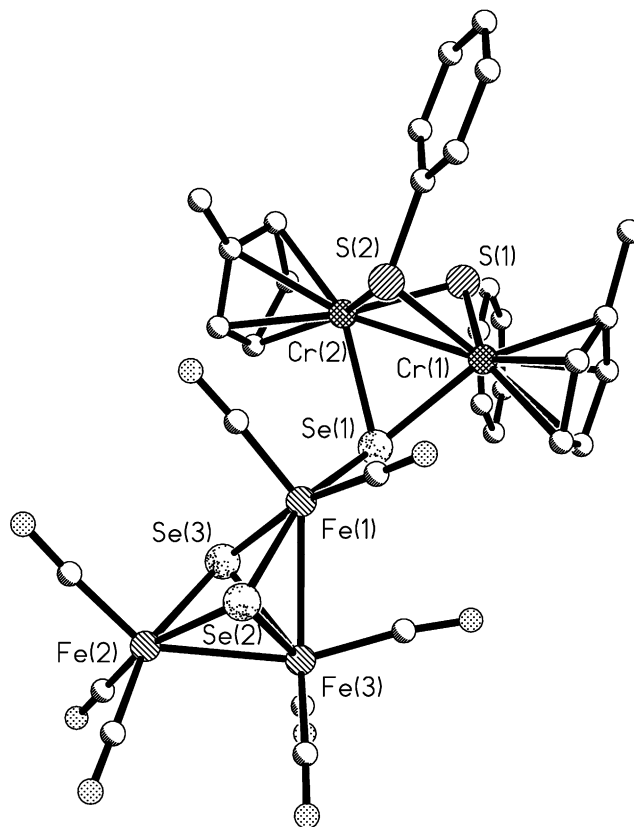


Fig. 1. Molecular structure of complex 2.

temperature gives the adduct  $[\text{Cp}^*\text{Cr}(\mu\text{-SPh})_2(\mu_3\text{-Se})\text{Fe}_3(\mu_3\text{-Se})_2(\text{CO})_8]$  (2) which was structurally characterized by means of single-crystal X-ray diffraction analysis (Fig. 1, Tables 2 and 3):

Table 1  
Types of complexes and  $-2J$  values

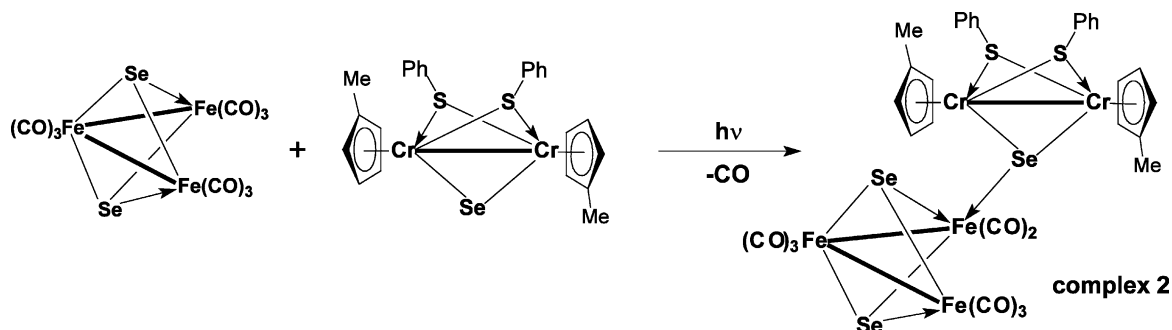
ML	$-2J$	ML	$-2J$	ML	$-2J$
$\text{Mo}(\text{CO})_5$ [8]	$440\text{ cm}^{-1}$	$\text{Mn}_2(\text{CO})_9$ [9]	$400\text{ cm}^{-1}$	$[\text{Me}_3\text{Pt}(\mu\text{-I})_2]$ [4]	$202\text{ cm}^{-1}$
$\text{W}(\text{CO})_5$ [8]	$440\text{ cm}^{-1}$	$\text{Re}_2(\text{CO})_9$ [10]	$424\text{ cm}^{-1}$	$[\text{W}(\text{CO})_2(\text{NO})\text{I}]_2$ [11]	$338\text{ cm}^{-1}$

Table 2  
Crystal data and structure refinement for **2–4**

	<b>2</b>	<b>3</b>	<b>4</b>
Empirical formula	C <sub>32</sub> H <sub>24</sub> Cr <sub>2</sub> Fe <sub>3</sub> O <sub>8</sub> S <sub>2</sub> Se <sub>3</sub>	C <sub>33</sub> H <sub>24</sub> Cr <sub>2</sub> Mn <sub>2</sub> O <sub>9</sub> S <sub>2</sub> Se <sub>1/2</sub> (C <sub>4</sub> H <sub>10</sub> O)	C <sub>32</sub> H <sub>24</sub> Cr <sub>2</sub> Mn <sub>2</sub> O <sub>8</sub> S <sub>2</sub> Se
Formula weight	1109.06	958.54	893.47
Diffractometer	Smart 1000 CCD	Smart 1000 CCD	Siemens P3
Temperature (K)	110(2)	293(2)	293(2)
Radiation, $\lambda$ (Mo–K $\alpha$ ) (Å)	0.71073	0.71073	0.71073
Crystal system	Monoclinic	Monoclinic	Monoclinic
Space group	<i>P</i> 2 <sub>1</sub> / <i>n</i>	<i>P</i> 2 <sub>1</sub> / <i>n</i>	<i>C</i> <i>c</i>
Unit cell dimensions			
<i>a</i> (Å)	10.532(3)	11.0719(7)	16.032(3)
<i>b</i> (Å)	25.344(1)	15.712(1)	13.766(3)
<i>c</i> (Å)	13.581(5)	21.601(1)	16.377(3)
$\beta$ (°)	94.72(2)	96.943(1)	104.72(1)
<i>V</i> (Å <sup>3</sup> )	3613(2)	3730.2(4)	3496(1)
<i>Z</i>	4	4	4
$\rho_{\text{calc}}$ (g cm <sup>-3</sup> )	2.039	1.707	1.698
Linear absorption, $\mu$ (cm <sup>-1</sup> )	49.45	23.70	25.19
Absorption correction	Semiempirical from equivalents	Semiempirical from equivalents	$\psi$ -curve
<i>F</i> (000)	2160	1916	1776
<i>T</i> <sub>max</sub> / <i>T</i> <sub>min</sub>	0.752/0.443	0.838/0.753	0.852/0.673
Scan type	$\omega$ -scan 0.3°/10 s exposure per frame	$\omega$ -scan 0.3°/10 s exposure per frame	$\theta/2\theta$
$\theta$ Range (°)	1.61–30.05	1.61–28.95	1.98–25.05
Measured	42203	23121	3167
Unique	10445 [ <i>R</i> <sub>int</sub> = 0.0524]	9027 ( <i>R</i> <sub>int</sub> = 0.0323)	3167 ( <i>R</i> <sub>int</sub> = 0.0215)
With [ <i>I</i> > 2 $\sigma$ ( <i>I</i> )]	6686	5871	2442
Parameters	453	571	427
Final <i>R</i> ( <i>F</i> <sub>hkl</sub> ): <i>R</i> <sub>1</sub>	0.0358	0.0406	0.0647
<i>wR</i> <sub>2</sub>	0.0675	0.1007	0.1517
GOF	0.972	0.810	0.974
$\rho_{\text{max}}/\rho_{\text{min}}$ (e Å <sup>-3</sup> )	0.881/–0.632	1.505/–0.415	1.623/–1.437

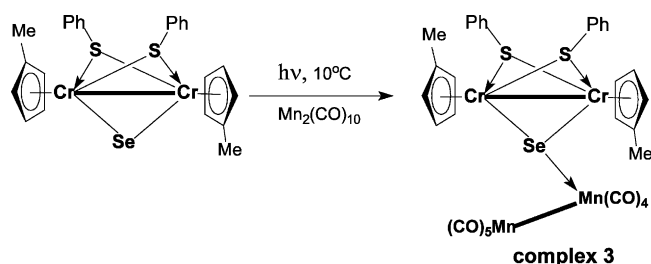
Table 3  
Selected bond lengths (Å) and bond angles (°) for **2–4**

<b>2</b>	<b>3</b>	<b>4</b>	
<i>Bond lengths</i>			
Cr(1)–Cr(2)	2.763(1)	Cr(1)–Cr(2) 2.7620(7)	Cr(1)–Cr(2) 2.816(3)
Cr(1)–Se(1)	2.4483(9)	Se(1)–Cr(1) 2.4593(6)	Cr(1)–Se(1) 2.463(2)
Cr(2)–Se(1)	2.4560(8)	Se(1)–Cr(2) 2.4469(6)	Cr(2)–Se(1) 2.464(3)
Fe(1)–Se(2)	2.320(1)	Cr(1)–S(1) 2.360(1)	Cr(1)–S(1) 2.375(4)
Fe(1)–Se(3)	2.3493(8)	Cr(1)–S(2) 2.359(1)	Cr(2)–S(1) 2.379(5)
Fe(1)–Se(1)	2.4648(9)	Se(1)–Mn(1) 2.5506(6)	Cr(1)–S(2) 2.343(4)
Fe(2)–Se(2)	2.3595(8)	Mn(1)–Mn(2) 2.9502(7)	Cr(2)–S(2) 2.344(4)
Fe(2)–Se(3)	2.374(1)		Se(1)–Mn(2) 2.413(2)
Fe(3)–Se(2)	2.366(1)		Se(1)–Mn(1) 2.425(3)
Fe(3)–Se(3)	2.3758(8)		Mn(1)–Mn(2) 2.835(3)
Fe(2)–Fe(3)	2.6184(9)		
Fe(1)–Fe(3)	2.706(1)		
<i>Bond angles</i>			
Cr(1)–Se(1)–Cr(2)	68.58(3)	Cr(2)–Se(1)–Cr(1) 68.52(2)	Mn(2)–Se(1)–Mn(1) 71.75(9)
Cr(1)–Se(1)–Fe(1)	114.56(3)	Cr(2)–S(1)–Cr(1) 71.82(3)	Mn(2)–Se(1)–Cr(1) 136.05(9)
Cr(2)–Se(1)–Fe(1)	112.53(3)	Cr(1)–S(2)–Cr(2) 71.54(3)	Mn(1)–Se(1)–Cr(1) 126.72(1)
Fe(1)–Se(2)–Fe(2)	97.84(3)	Cr(1)–S(2)–Cr(2) 71.54(3)	Mn(2)–Se(1)–Cr(2) 139.5(1)
Fe(1)–Se(2)–Fe(3)	70.53(2)		Mn(1)–Se(1)–Cr(2) 122.61(8)
Fe(2)–Se(2)–Fe(3)	67.29(3)		Cr(1)–Se(1)–Cr(2) 69.71(7)
Fe(1)–Se(3)–Fe(2)	96.66(3)		Cr(1)–S(2)–Cr(2) 73.9(1)
Fe(1)–Se(3)–Fe(3)	69.88(3)		
Fe(2)–Se(3)–Fe(3)	66.92(2)		

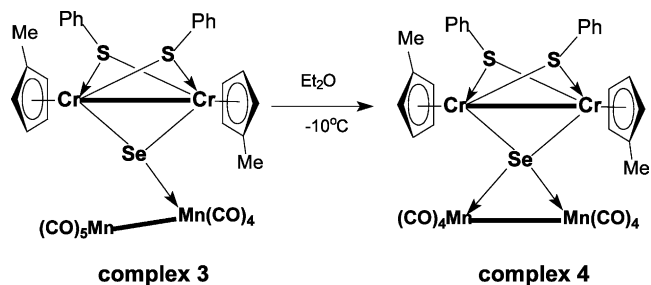


The geometry of  $\text{Fe}_3(\mu_3\text{-Se})_2(\text{CO})_8$  fragment does not undergoes significant changes in comparison with the initial  $\text{Fe}_3(\mu_3\text{-Se})_2(\text{CO})_9$  [13]. The length of Cr(1)–Cr(2) bond (2.763(1) Å) and the value of angle Cr(1)–Se(1)–Cr(2) ( $68.58(3)^\circ$ ) are close to those for complex **1** but Cr–Se bonds (2.4483(9) and 2.4560(8) Å) are elongated in comparison with **1** (Cr–Se 2.401 and 2.396 Å) and this elongation could be the reason of the decreasing of the exchange parameter of **2** ( $-2J = 256 \text{ cm}^{-1}$ ):  $\mu_{\text{eff}}$  reduced from  $1.8\mu_{\text{B}}$  (287 K) to  $0.42\mu_{\text{B}}$  (79 K) with respect to  $578 \text{ cm}^{-1}$  for **1**.

The photochemical interaction between **1** and  $\text{Mn}_2(\text{CO})_{10}$  at the room temperature gives black crystals of  $[\text{Cp}^*\text{Cr}(\mu\text{-SPh})_2(\mu_3\text{-Se})\text{Mn}_2(\text{CO})_9]$  (**3**) studied by X-ray analysis (Fig. 2, Tables 2 and 3).



Selenium atom is coordinated to only one of manganese atoms (Mn–Se 2.5506(6) Å). The Mn–Mn and Cr–Cr bond lengths (2.920 and 2.762 Å, respectively) remain almost unchanged in comparison with initial compounds, while significant elongation of Cr–Se bonds up to 2.447 and 2.460 Å takes place. The similar elongation of Cr–Se bonds was observed in **2** and in the known cluster  $\text{Cp}_2\text{Cr}_2(\mu\text{-SPh})_2\text{SeCr}(\text{CO})_5$  [14]. This Cr–Se bond elongation in **3** is accompanied by decreasing of its  $-2J$  value to  $230 \text{ cm}^{-1}$  ( $\mu_{\text{eff}}$  reduced from 1.68 down to  $0.56\mu_{\text{B}}$  in the 295–80 K temperature range) with respect to  $578 \text{ cm}^{-1}$  for **1**. It is noteworthy that  $-2J$  values for all adducts  $\text{Cp}_2\text{Cr}_2(\mu\text{-SCMe}_3)_2(\mu\text{-S})\text{-ML}$  (Table 1) are near  $400\text{--}440 \text{ cm}^{-1}$  [3], e.g. very close to  $430 \text{ cm}^{-1}$  for the initial  $\text{Cp}_2\text{Cr}_2(\mu\text{-SCMe}_3)_2(\mu\text{-S})$  [2]. It means that antiferromagnetic exchange interactions in selenide-bridged complexes are more sensitive to the nature of chalcogen atom than in the case of sulfide-bridged complexes.



Keeping of the ether solution of **3** at  $-10^\circ\text{C}$  for 48 h favours the further decarbonylation with the formation

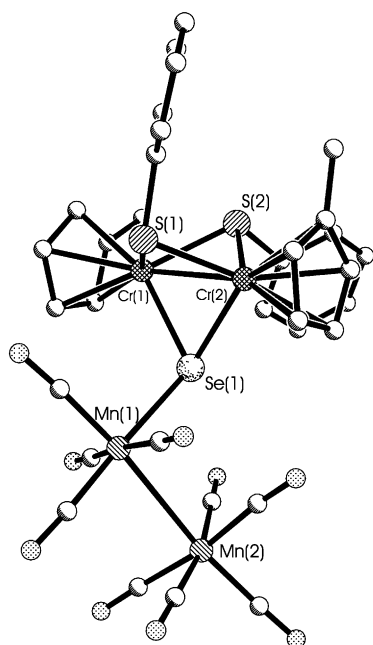


Fig. 2. Molecular structure of complex **3**.

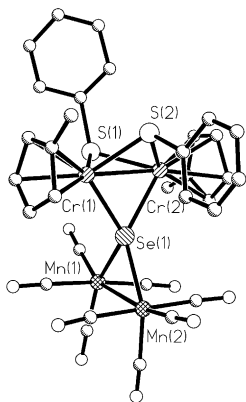


Fig. 3. Molecular structure of complex **4**.

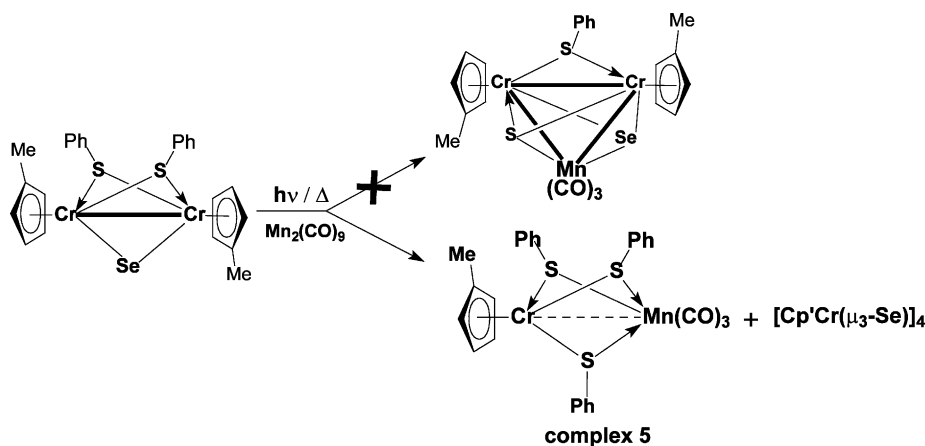
of a new cluster  $[\text{Cp}'\text{Cr}(\mu\text{-SPh})]_2(\mu_4\text{-Se})\text{Mn}_2(\text{CO})_8$  (**4**) which was characterized by X-ray analyses (Fig. 3, Tables 2 and 3) and has a spirane-like metal-chalcogenide core where  $\mu_4\text{-Se}$  atom is coordinated with two chromium ( $\text{Cr}\text{-Cr}$  2.816(3) Å,  $\text{Cr}\text{-Se}$  av. 2.464 Å) and two manganese atoms ( $\text{Mn}\text{-Mn}$  2.835(3) Å,  $\text{Mn}\text{-Se}$  av. 2.419 Å).

Due to an elongation of  $\text{Cr}\text{-Cr}$  bond in **4** with respect to 2.76 Å in **3** one could expect decreasing of  $-2J$  value but its unexpected increasing up to  $324\text{ cm}^{-1}$  ( $\mu_{\text{eff}}$  reduced from  $1.51\mu_{\text{B}}$  down to  $0.53\mu_{\text{B}}$  in the 292–79 K temperature range) was observed. The reason is still not clear. We could only suppose that it is a result of some

place the significant decreasing of  $-2J$  values in comparison with  $\mu_3\text{-S}$ -containing clusters, particularly containing  $\text{Mn}_2(\text{CO})_9$  group (Table 1). Probably some role could play the presence of  $\text{Mn}\text{-Mn}$  bond in **4** whereas known  $\mu_4\text{-S}$ -containing clusters had two ML groups linked by two iodine bridges only without  $\text{M}\text{-M}$  bond between them (Table 1).

The conservation of the structure of **1** during the photochemical inter-reaction with  $\text{Fe}_3(\mu_3\text{-Se})_2(\text{CO})_9$  or  $\text{Mn}_2(\text{CO})_{10}$  and formation of the adducts **2–4** is in contrast to the known photochemical transformations of  $\text{Cp}_2\text{Cr}_2(\mu\text{-SCMe}_3)_2(\mu\text{-S})$  into pentanuclear metal-spirane cluster  $\text{Cp}_2\text{Cr}_2(\mu\text{-SCMe}_3)(\mu_3\text{-S})_2\text{Fe}(\mu_3\text{-S})_2\text{Fe}_2(\text{CO})_9$  [15] and triangular cluster  $\text{Cp}_2\text{Cr}_2(\mu\text{-SCMe}_3)(\mu_3\text{-S})_2\text{Mn}(\text{CO})_3$  [16], respectively. Probably this difference results from the longer distance between ML group and chromium atoms in the presence of bulky selenide bridge in comparison with sulfide bridge, on one hand, and on the other hand — the stronger  $\text{S}\text{-Ph}$  bond in respect to  $\text{S}\text{-CMe}_3$  bond, does not favour the elimination of  $\text{CMe}_3$  accompanying the transformation of  $\text{SPh}$  into  $\mu_3\text{-S}$  bridging ligand.

The photochemical reaction of **1** and  $\text{Mn}_2(\text{CO})_{10}$  at higher temperature (in refluxing benzene) unexpectedly leads to  $\text{Cp}'\text{Cr}(\mu\text{-SPh})_3\text{Mn}(\text{CO})_3$  (**5**) instead of triangular  $\text{Cp}'_2\text{Cr}_2(\mu\text{-SPh})(\mu_3\text{-Se})(\mu_3\text{-S})\text{Mn}(\text{CO})_3$  supposed by analogy with known  $\text{Cp}_2\text{Cr}_2(\mu\text{-SCMe}_3)(\mu_3\text{-S})_2\text{Mn}(\text{CO})_3$  [16,17].



electronic features of  $\mu_4\text{-Se}$  atom which has no lone pair (particularly, in **4** the significant shortening of the  $\text{Mn}\text{-Se}$  bond lengths (av. 2.418(3) Å) takes place in comparison with  $\text{Mn}\text{-Se}$  distance (2.5506(6) Å in **3**). But in the case of two known clusters with  $\mu_4\text{-S}$ -bridge atom took

According to the X-ray data (Fig. 4, Tables 4 and 5) the  $\text{Cr}(1)\text{-Mn}(1)$  bond (3.0239(7) Å) has probably an order 0.5 in accordance with the observed paramagnetic properties of **5** — three unpaired electrons ( $\mu_{\text{eff}}$  (3.67 $\mu_{\text{B}}$ ) does not depend on the temperature).

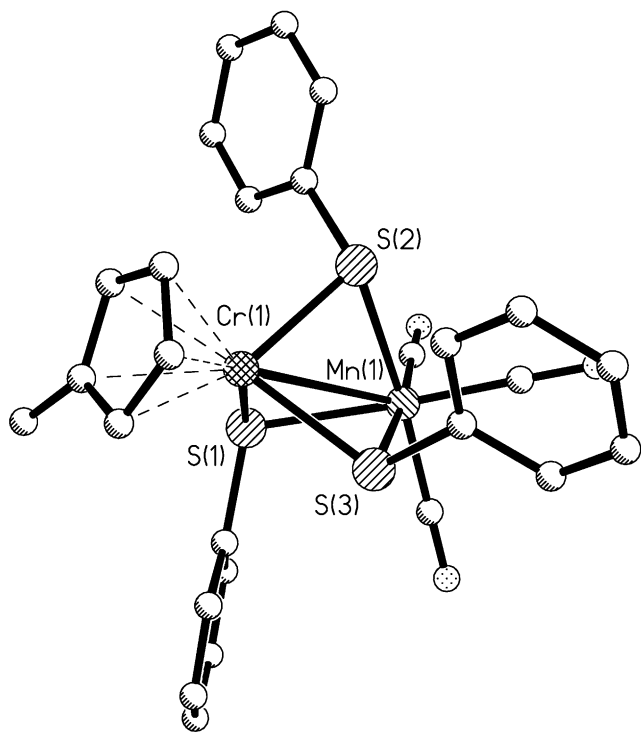
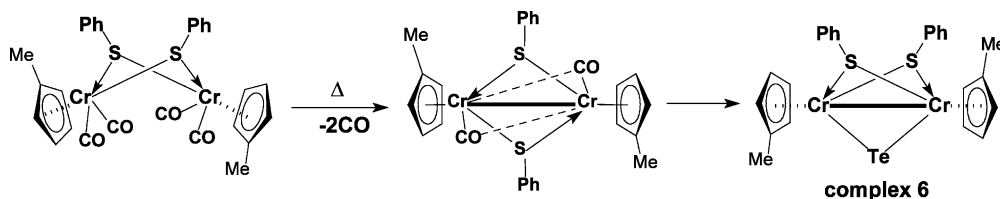


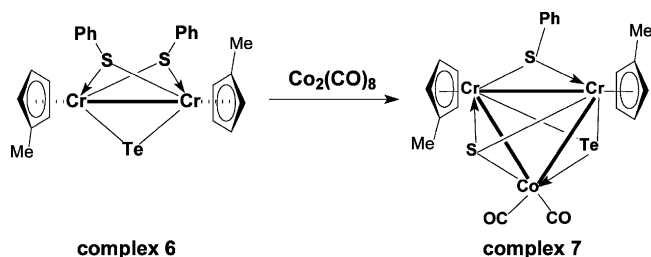
Fig. 4. Molecular structure of complex 5.

The Te-bridged binuclear chromium complex  $[\text{Cp}^*\text{Cr}(\mu\text{-SPh})_2](\mu\text{-Te})$  (**6**) was prepared by the reaction of elemental tellurium with  $[\text{Cp}^*\text{Cr}(\text{CO})(\mu\text{-SPh})]_2$  which was obtained while the decarbonylation of  $[\text{Cp}^*\text{Cr}(\text{CO})_2(\mu\text{-SPh})]_2$ :



The structure of the black crystals of **6** was studied by single-crystal X-ray diffraction analyses (Fig. 5, Tables 4 and 5). It contains two  $\text{Cp}^*\text{Cr}$  groups linked by direct Cr–Cr bond (2.772(3) Å), two thiolate bridge groups (Cr–S av. 2.359 Å) and one telluride bridge atom (Cr–Te 2.601(2)–2.607(2) Å, Cr–Te–Cr 64.30(7)°). Complex **6** is unstable and it was impossible to get the clear data on its magnetic properties.

The reaction of **6** with  $\text{Co}_2(\text{CO})_8$  gives mixed-metal heterochalcogenic cluster  $[\text{Cp}'_2\text{Cr}_2(\mu\text{-SPh})(\mu_3\text{-S})(\mu_3\text{-Te})\text{Co}(\text{CO})_2]$  (**7**) as diamagnetic brown crystals which are stable under argon.



Single-crystal X-ray diffraction analysis of **7** (Fig. 6, Tables 4 and 5) demonstrated the similarity of its core to those found earlier for  $\text{Cp}'_2\text{Cr}_2(\text{SR})(\mu_3\text{-S})(\mu_3\text{-X})\text{Co}(\text{CO})_2$  (X = S; R =  $\text{CMe}_3$  (**8**) [8] or X = Se; R = Ph (**9**) [1]). In **7**  $\mu_3$ -telluride and  $\mu_3$ -sulfide bridging atoms are situated over and under  $\text{Cr}_2\text{Co}$  triangle (Cr–S 2.299(1) Å, Co–S 2.199(1) Å, Cr–Te 2.6303(9) Å, Co–Te 2.466(1) Å). Diamagnetic properties of **7** are unexpected because the metal–metal bonds (Cr–Cr 2.646(1) Å, Cr–Co 2.628(1) Å) in **7** are elongated in respect to **8** (Cr–Cr 2.590 Å, Cr–Co 2.530 and 2.569 Å) and **9** (Cr–Cr 2.624 Å, Cr–Co av. 2.612 Å) which appeared antiferromagnetic properties. Apparently in **7** the super-exchange interactions via tellurium atom are more important than direct spin–spin interactions via M–M bonds.

### 3. Experimental

All manipulations were carried out in pure argon atmosphere with using of absolute solvents. Commercial  $\text{Mn}_2(\text{CO})_{10}$  was recrystallized from hexane.

$[\text{Cp}'\text{Cr}(\text{CO})_3]_2$  was prepared in accord with [18].  $\text{Fe}_3(\text{CO})_9(\text{Se})_2$  was prepared as in Ref. [19]. IR-spectra were recorded at 'Specord-75 IR' in KBr pellets. Differential scanning calorimetry (DSC) was studied with thermoanalyser 'Mettler' TA-3000 in dry argon.

The temperature dependence of the magnetic susceptibilities ( $\chi_m$ ) of the investigated compounds was determined by the Faraday technique between 77 and 296 K using original device [20]. The effective magnetic moments of compounds were calculated by formula (1)

$$\mu_{\text{eff}} = 797.7(B_m T)^{1/2} \quad (1)$$

Table 4  
Crystal data and structure refinement for 5–7

	5	6	7
Empirical formula	C <sub>27</sub> H <sub>22</sub> CrMnO <sub>3</sub> S <sub>3</sub>	C <sub>24</sub> H <sub>24</sub> Cr <sub>2</sub> S <sub>2</sub> Te	C <sub>20</sub> H <sub>19</sub> CoCr <sub>2</sub> O <sub>2</sub> S <sub>2</sub> Te
Formula weight	597.57	608.15	646.00
Diffractometer	Smart 1000 CCD	Siemens P3	Smart 1000 CD
Temperature (K)	190(2)	298(2)	110(2)
Radiation, $\lambda$ (Mo–K $\alpha$ ) (Å)	0.71073	0.71073	0.71073
Crystal system	Orthorhombic	Monoclinic	Monoclinic
Space group	<i>Pbca</i>	<i>P2<sub>1</sub>/n</i>	<i>P2<sub>1</sub>/c</i>
Unit cell dimensions			
<i>a</i> (Å)	14.5207(9)	12.447(6)	10.220(3)
<i>b</i> (Å)	18.623(1)	13.827(7)	16.187(5)
<i>c</i> (Å)	19.380(1)	13.719(7)	13.373(4)
$\beta$ (°)	90	92.24(4)	101.07(3)
<i>V</i> (Å <sup>3</sup> )	5240.5(5)	2359.4(19)	1636.3(9)
<i>Z</i>	8	4	4
$\rho_{\text{calc}}$ (g cm <sup>-3</sup> )	1.515	1.712	1.681
Linear absorption, $\mu$ (cm <sup>-1</sup> )	11.63	23.18	32.61
Absorption correction	Semiempirical from equivalents	$\psi$ -curve	Empirical from equivalents
<i>F</i> (000)	2440	1200	1256
<i>T</i> <sub>max</sub> / <i>T</i> <sub>min</sub>	0.967/0.77	0.756/0.643	0.801/0.543
Scan type	$\omega$ -scan 0.3°/10 s exposure per frame	$\theta/2\theta$	$\omega$ -scan with 0.3°/10 s exposure per frame
$\theta$ Range (°)	2.07–29.06	2.62–20.04	2.61–27.52
Measured	38037	2099	20742
Unique	6973 ( <i>R</i> <sub>int</sub> = 0.0543)	1974 ( <i>R</i> <sub>int</sub> = 0.0434)	4966 ( <i>R</i> <sub>int</sub> = 0.0477)
With [ <i>I</i> > 2 $\sigma$ ( <i>I</i> )]	3757	1577	3353
Parameters	404	262	329
Final <i>R</i> ( <i>F</i> <sub>hkl</sub> ): <i>R</i> <sub>1</sub>	0.0472	0.0447	0.0367
<i>wR</i> <sub>2</sub>	0.1000	0.1136	0.0833
GOF	0.977	1.027	0.980
$\rho_{\text{max}}/\rho_{\text{min}}$ (e Å <sup>-3</sup> )	1.008/–0.315	0.579/–0.464	1.110/–1.076

The best-fit of the values was obtained with the Heisenberg–Dirak–Van Vleck (HDVV) theoretical

model for two exchange-coupled paramagnetic ions in the absence of orbital degeneracy of the complex ground

Table 5  
Selected bond lengths (Å) and bond angles (°) for 5–7

5	6	7
<i>Bond lengths</i>		
Cr(1)–S(2)	2.3429(8)	Cr(2)–Te(1) 2.618(1)
Cr(1)–S(1)	2.3591(9)	Cr(1)–Te(1) 2.630(1)
Cr(1)–S(3)	2.3711(9)	Cr(1)–S(1) 2.282(2)
Cr(1)–Mn(1)	3.0239(7)	Cr(1)–S(2) 2.335(1)
Mn(1)–S(2)	2.3985(8)	Cr(2)–S(1) 2.290(1)
Mn(1)–S(1)	2.3997(9)	Cr(2)–S(2) 2.333(1)
Mn(1)–S(3)	2.4210(8)	Cr(1)–Co(1) 2.628(1)
		Cr(2)–Co(1) 2.623(1)
		Co(1)–S(1) 2.199(1)
		Te(1)–Co(1) 2.466(1)
<i>Bond angles</i>		
Cr(1)–S(1)–Mn(1)	78.90(3)	Cr(2)–Te(1)–Cr(1) 60.56(3)
Cr(1)–S(2)–Mn(1)	79.24(3)	Cr(1)–S(1)–Cr(2) 70.55(5)
Cr(1)–S(3)–Mn(1)	78.24(3)	Cr(2)–S(2)–Cr(1) 69.05(4)
		Co(1)–Te(1)–Cr(2) 62.03(3)
		Co(1)–Te(1)–Cr(1) 61.97(3)
		Co(1)–S(1)–Cr(1) 71.77(4)
		Co(1)–S(1)–Cr(2) 71.28(4)



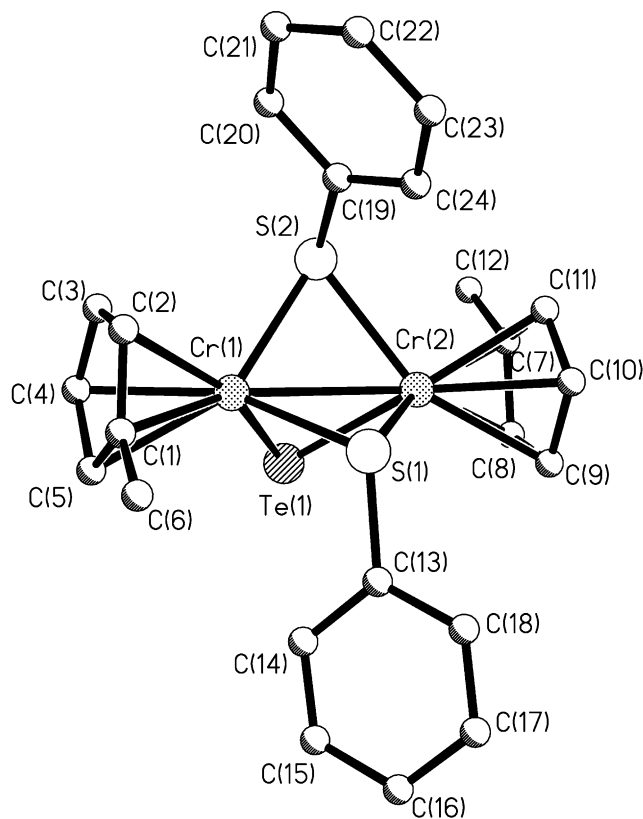


Fig. 5. Molecular structure of complex 6.

states. The spin Hamiltonian has the form (2)

$$H = -2JS_1S_2 + g\beta H(S_{1z} + S_{2z}) \quad (2)$$

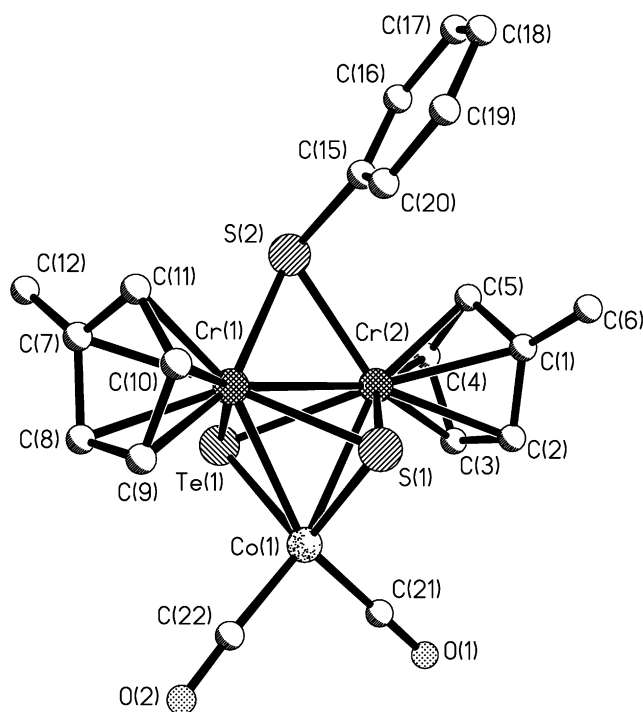


Fig. 6. Molecular structure of complex 7.

where  $J$  is the isotropic exchange parameter,  $g$  is the isotropic  $g$  factor and  $S$  are the spins of the exchange coupled ions. The calculation of the theoretical  $\mu_{\text{eff}}$  values and the least-squares treatment were carried as reported [21].

Crystal structures were solved by direct method and refined in full-matrix anisotropic–isotropic (H-atoms) approximation. All calculations were carried out with the complex of programs SHELXTL PLUS 5 [22]. The important crystallographic data and refinement parameters for 2–7 are given in Tables 2 and 4. The most important bond lengths and angles of the complexes 2–7 are presented in the Tables 3 and 5.

### 3.1. Preparation of $\text{Cp}'_2\text{Cr}_2(\text{SPh})_2\text{SeFe}_3\text{Se}_2(\text{CO})_8$ (2)

The solution of 0.15 g (0.26 mmol) of **1** and 0.15 g (0.26 mmol)  $\text{Fe}_3\text{Se}_2(\text{CO})_9$  in benzene (20 ml) was irradiated by UV-light for 9 h while stirring and cooling by running water. Resulting dark brown reaction mixture was evaporated to dryness and the residue was extracted with 25 ml of hexane and then with 30 ml of ether. To the ether solution 15 ml of hexane was added and both extracts were concentrated in vacuo to 1/4 of initial volume and kept at  $-18^\circ\text{C}$  for 48 h. Black–brown crystals were separated, washed by hexane and recrystallized from  $\text{Et}_2\text{O}$ +hexane (1:2) mixture. Yield 0.17 g (57%).

IR-spectra ( $\text{cm}^{-1}$ ): 584 w, 608 w, 688 w, 744 w, 816 w, 800 m, 1952 m, 1976 s, 1990 s, 2016 s, 2048 s. Anal. Found: C, 34.58; H, 2.16; S, 6.27; (DSC) CO, 20.2.  $\text{C}_6\text{H}_5$  13.9;  $\text{Cp}'$  14.3. Residue after pyrolyses:  $\text{Cr}_2\text{Fe}_3\text{S}_2\text{Se}_3$ .  $\text{C}_{32}\text{H}_{24}\text{S}_2\text{Se}_3\text{Cr}_2\text{Fe}_3\text{O}_8$ . Calc.: C, 34.66; H, 2.18; S, 5.78; CO, 20.0;  $\text{C}_6\text{H}_5$ , 13.6;  $\text{Cp}'$ , 14.4%.

The single crystals of **2** were used for X-ray analysis.

### 3.2. Preparation of $\text{Cp}'_2\text{Cr}_2(\mu\text{-SPh})_2(\mu_3\text{-Se})\text{Mn}_2(\text{CO})_9$ (3)

The solution of 0.5 g (0.89 mmol) of **1** and 0.4 g (0.96 mmol) of  $\text{Mn}_2(\text{CO})_{10}$  in benzene (30 ml) was irradiated by UV-light for 1.5 h while stirring and cooling by running water. Reaction mixture was evaporated to dryness and the residue was extracted with 30 ml of  $\text{Et}_2\text{O}$ . Hexane (10 ml) was added to extract, the mixture was concentrated until the beginning of crystallization and kept at  $-10^\circ\text{C}$  for 12 h. Black needle-like crystals were dried in vacuo. Yield 0.45 g (54%).

IR ( $\text{cm}^{-1}$ ): 2960 w, 2920 w, 2360 w, 2072 s, 2000 s, 1975 s, 1936 s, 1905 s, 1665 w, 1576 m, 1470 w, 1065 w, 1025 w, 1000 w, 825 s, 745 s, 688 m, 650 s, 615 m, 480 m, 410 m. Anal. Found: C, 43.12; H, 3.87; S, 7.09. Calc. for  $\text{C}_{33}\text{H}_{24}\text{S}_2\text{SeCr}_2\text{Mn}_2\text{O}_9$ : C, 43.01; H, 2.63; S, 6.96%.

The single crystals of **3** were used for X-ray analysis.



### 3.3. Preparation of $Cp'_2Cr_2(\mu-SPh)_2(\mu-Se)Mn_2(CO)_8$ (**4**)

A mother solution left after precipitation of **3** was evaporated to dryness, extracted with 20 ml of  $Et_2O$ , concentrated to 20 ml after addition of 10 ml of hexane and then kept at  $-10^\circ C$  for 48 h. Black–green crystals were separated, washed with hexane and dried in vacuo. Yield 0.08 g (10%). IR ( $cm^{-1}$ ): 2045 m, 1970 s, 1925 s, 1900 s, 825 m, 740 s, 700 w, 655 m, 620 s.

The single crystals of **4** recrystallized from  $CH_2Cl_2$  + hexane were used for X-ray analysis.

### 3.4. Preparation of $Cp'Cr(\mu-SPh)_3Mn(CO)_3$ (**5**)

The solution of 0.3 g (0.53 mmol) of **1** and 0.2 g (0.51 mmol) of  $Mn_2(CO)_{10}$  in boiling benzene (20 ml) was irradiated by UV-light for 2 h. Reaction mixture was evaporated to dryness, washed with 10 ml of hexane and the residue was extracted with 40 ml of ether. To this extract 10 ml of hexane was added and the solution was concentrated in vacuo to 20 ml and kept at  $-10^\circ C$  for 12 h to give black prisms washed with hexane and dried in vacuo. Yield 0.05 g (23%). IR (KBr,  $cm^{-1}$ ): 2010 s, 1930 s, 1905 s, 1020 w, 820 m, 740 s, 690 m, 620 m.

The single crystal of **5** was used for X-ray analysis.

### 3.5. Preparation of $[Cp'Cr(\mu-SPh)]_2(\mu-Te)$ (**6**)

#### 3.5.1. Preparation of $[Cp'Cr(CO)(\mu-SPh)]_2$

$Ph_2S_2$  (1.06 g, 4.8 mmol) was added to the green solution of 2.1 g (4.8 mmol)  $[Cp'Cr(CO)_3]_2$  in 50 ml of hexane at  $0^\circ C$  and was stirred for 0.5 h. Resulting dark-orange solution was refluxed for 1 h until the disappearing of intermediate  $[Cp'Cr(CO)_2]_2(\mu-SPh)_2$  (TLC, Silufol: orange spot,  $R_f$  –0.6 in benzene). Black crystalline precipitate was filtered from green solution, extracted with  $CH_2Cl_2$  and after evaporation of cherry-brown solution the resulting tar was crystallized at the treating by benzene. The solid substance was separated, washed by hexane and dried in vacuo. Yield  $[Cp'Cr(CO)(\mu-SPh)]_2$  0.35 g (37%). IR spectra ( $cm^{-1}$ ): 1870 s, 810 m, 730 s, 680 m.

#### 3.5.2. The reaction of $[Cp'Cr(CO)(\mu-SPh)]_2$ with Te

To the solution of 0.35g (0.65 mmol)  $Cp'Cr(CO)(\mu-SPh)]_2$  in 50 ml of THF 0.14 g (1.1mmol) of Te powder was added and the mixture was stirred for 18 h at the room temperature (r.t.). The green–brown mixture was evaporated to dryness, washed with 20 ml of hexane, extracted with 20 ml of  $CH_2Cl_2$  and filtered. The addition of hexane gave black crystals which were washed by hexane and dried in vacuum. Yield 0.1 g (23%). IR spectra ( $cm^{-1}$ ): 1080 m, 1020 m, 810 s, 730 s, 680 m.

The single crystals of **6** were used for X-ray analysis.

### 3.6. Preparation of $Cp'_2Cr_2(\mu-PhS)(\mu-S)(\mu-Te)Co(CO)_2$ (**7**)

A violet solution of 0.1 g (0.16 mmol) of **6** in 10 ml  $CH_2Cl_2$  was added to the yellow–brown solution of 0.1 g (0.32 mmol)  $Co_2(CO)_8$  in 20 ml of  $CH_2Cl_2$ . The mixture was evaporated in vacuum, the residue was washed by 10 ml of hexane and extracted by 20 ml of  $Et_2O$ . This extract after addition of 10 ml of hexane was concentrated until the small quantity of brown precipitate forms. The solution was filtered and after addition of 5 ml of hexane was again concentrated to 3 ml and then kept at  $-10^\circ C$  for 12 h. Needle-like crystals of **6** were washed by cold hexane and dried in vacuo. Yield 0.02g (19%).

IR spectrum ( $cm^{-1}$ ): 1975 s, 1935 s, 830 m, 735 w, 535 w. Anal. Found: C, 36.82; H, 3.41; S, 9.66. Calc. for  $C_{20}H_{19}S_2SeCr_2CoO_2$ : C, 37.21; H, 2.94; S, 9.92%.

The single crystal of **7** was used for X-ray analysis.

## 4. Supplementary material

Crystallographic data for the structural analysis have been deposited with the Cambridge Crystallographic Data Centre, CCDC nos. 183565 (**2**), 183564 (**3**), 183566 (**4**), 183567 (**5**), 172670 (**6**) and 172671 (**7**). Copies of this information may be obtained free of charge from The Director, CCDC, 12 Union Road, Cambridge CB2 1EZ, UK (Fax: +44-1223-336033; e-mail: deposit@ccdc.cam.ac.uk or www: <http://www.ccdc.cam.ac.uk>).

## Acknowledgements

We thank Dr. Zh.V. Dobrokhotova for the differential scanning calorimetric study and Russian Foundation of Basic Research (grants 02-03-33075, 00-03-32626, 02-03-06170, 02-03-06171) for financial support.

## References

- [1] A.A. Pasynskii, F.S. Denisov, Yu.V. Torubaev, N.I. Semenova, V.M. Novotortsev, O.G. Ellert, S.E. Nefedov, K.A. Lyssenko, J. Organomet. Chem. 612 (2000) 9.
- [2] A.A. Pasynskii, I.L. Eremenko, Yu.V. Rakitin, V.M. Novotortsev, V.T. Kalinnikov, G.G. Aleksandrov, Yu.T. Struchkov, J. Organomet. Chem. 165 (1979) 57.
- [3] A.A. Pasynskii, I.L. Eremenko, Usp. Khim. 58 (1989) 303 (in Russian).
- [4] A.A. Pasynskii, Yu.V. Torubaev, S.E. Nefedov, I.L. Eremenko, O.G. Ellert, V.K. Belsky, A.I. Stastch, J. Organomet. Chem. 536–537 (1997) 433.
- [5] Yu.V. Rakitin, A.A. Pasynskii, Zh. Neorg. Khim. 46 (2001) 966 (in Russian).
- [6] L.Y. Goh, M.S. Tay, T.C.W. Mak, R.J. Wang, Organometallics 11 (1992) 1711.

- [7] L.Y. Goh, M.S. Tay, C. Wei, *Organometallics* 13 (1994) 1813.
- [8] A.A. Pasynskii, I.L. Eremenko, B. Orazsakhov, *J. Organomet. Chem.* 210 (1981) 377.
- [9] A.A. Pasynskii, I.L. Eremenko, B. Orazsakhov, *J. Organomet. Chem.* 214 (1981) 351.
- [10] A.A. Pasynskii, I.L. Eremenko, S.E. Nefedov, B. Orazsakhov, A.A. Zharkikh, O.G. Ellert, V.M. Novotortsev, A.I. Yanovsky, Yu.T. Struchkov, *J. Organomet. Chem.* 444 (1993) 101.
- [11] I.L. Eremenko, V.M. Novotortsev, I.A. Petrunenko, H. Berke, *Izv. Ross. Akad. Nauk, Ser. Khim.* (1995) 1 (in Russian).
- [12] A.A. Pasynskii, I.L. Eremenko, B. Orazsakhov, G.Sh. Gasanov, V.M. Novotortsev, O.G. Ellert, Z.M. Seifullina, V.E. Shklover, Yu.T. Struchkov, *J. Organomet. Chem.* 270 (1984) 53.
- [13] R. Seidel, B. Schnautz, G. Henkel, *Angew. Chem. Int. Ed. Engl.* 35 (1996) 1710.
- [14] L.Y. Goh, M.S. Tay, Y.Y. Lim, W. Chen, Z. Zhou, T.C.W. Mak, *J. Organomet. Chem.* 441 (1992) 51.
- [15] I.L. Eremenko, A.A. Pasynskii, A.S. Katugin, V.R. Zalmanovich, B. Orazsakhov, S.A. Sleptsova, A.I. Nekhaev, V.V. Kaverin, O.G. Ellert, V.M. Novotortsev, A.I. Yanovsky, V.E. Shklover, Yu.T. Struchkov, *J. Organometal. Chem.* 365 (1989) 325.
- [16] A.A. Pasynskii, I.L. Eremenko, B. Orazsakhov, G.Sh. Gasanov, V.M. Novotortsev, O.G. Ellert, Z.M. Seifullina, V.E. Shklover, Yu.T. Struchkov, *J. Organometal. Chem.* 270 (1984) 53.
- [17] S.E. Nefedov, A.A. Pasynskii, I.L. Eremenko, B. Orazsakhov, V.M. Novotortsev, O.G. Ellert, A.F. Shestakov, A.I. Yanovsky, Yu.T. Struchkov, *J. Organomet. Chem.* 384 (1989) 279.
- [18] R. Birdwhistell, P. Hackett, A.R. Manning, *J. Organomet. Chem.* 157 (1978) 239.
- [19] W. Hieber, J. Gruber, *Z. Anorg. Allg. Chem.* B296 (1958) 91.
- [20] V.M. Novotortsev, PhD thesis, Institute of General and Inorganic Chemistry, Moscow, 1974.
- [21] Yu.V. Rakitin, V.T. Kalinnikov, *Modern Magnetochemistry* (in Russian), Nauka, St. Petersburg, 1994, p. 272.
- [22] G.M. Sheldrick, *Crystallographic Computing 3: Data Collection, Structure Determination, Proteins and DataBases*, Clarendon Press, New York, 1985, p. 175.